Anal Bioanal Chem (2014) 406:5513–5520
DOI 10.1007/s00216-014-7975-5

NOTE

Ultrasensitive detection and identification of *BRAF* V600 mutations in fresh frozen, FFPE, and plasma samples of melanoma patients by E-*ice*-COLD-PCR

Alexandre How-Kit · Céleste Lebbé · Aurélie Bousard · Antoine Daunay · Nicolas Mazaleyrat · Christian Daviaud · Samia Mourah · Jörg Tost

Received: 2 April 2014 / Revised: 27 May 2014 / Accepted: 13 June 2014 / Published online: 27 June 2014

Abstract A number of molecular diagnostic methods have been developed for the detection and identification of mutations in tumor samples, which are important for the choice of treatment in the context of personalized medicine. For the treatment of metastatic melanoma, Vemurafenib is recommended for patients with *BRAF* V600 activating mutations. However, the different assays developed to date for the detection of these mutations lack sensitivity or specificity or do not allow a sequencing-based identification or validation of the mutation. Recently, enhanced improved and complete enrichment co-amplification at lower denaturation temperature-polymerase chain reaction (E-*ice*-COLD-PCR) has been developed as a sensitive method for the detection and identification of mutations in *KRAS* codons 12/13. Here, we present the first E-*ice*-COLD-PCR assay for the detection and identification of *BRAF* codon 600 mutations, which has a large dynamic range, as 25 pg to 25 ng can be used as DNA input without any reduction in mutation enrichment efficiency, and which can detect down to 0.01 % of mutated alleles in a wild-type background. The assay has been validated on fresh frozen, formalin-fixed paraffin-embedded (FFPE), and plasma samples of melanoma patients and has allowed the detection and identification of *BRAF* mutations present in samples appearing as wild type using standard pyrosequencing, endpoint genotyping, or Sanger sequencing. Thus, the *BRAF* V600 E-*ice*-COLD-PCR assay is currently one of the most powerful molecular diagnostic tools for the ultrasensitive detection and identification of *BRAF* codon 600 mutations.

Keywords E-*ice*-COLD-PCR · Melanoma · *BRAF* V600 mutation · Vemurafenib · Molecular diagnostics

Samia Mourah and Jörg Tost should be considered as senior coauthors.

Electronic supplementary material The online version of this article (doi:10.1007/s00216-014-7975-5) contains supplementary material, which is available to authorized users.

A. How-Kit · A. Daunay · J. Tost (✉)
Laboratory for Functional Genomics, Fondation Jean Dausset - CEPH, 75010 Paris, France
e-mail: tost@cng.fr

C. Lebbé
Département de Dermatologie France, AP-HP - Hôpital Saint-Louis, 75010 Paris, France

C. Lebbé
Université Paris-Diderot, Sorbonne Paris Cité, 75010 Paris, France

C. Lebbé
INSERM U976, 75010 Paris, France

A. Bousard · N. Mazaleyrat · C. Daviaud · J. Tost
Laboratory for Epigenetics and Environment, Centre National de Génotypage, CEA-Institut de Génomique, 91000 Evry, France

S. Mourah
Laboratoire de Pharmacologie-Génétique, AP-HP - Hôpital Saint-Louis, 75010 Paris, France

S. Mourah
INSERM UMR-S 940, 75010 Paris, France

Introduction

Activating mutations of the *BRAF* serine/threonine-protein kinase leading to a constant activation of the MAPK pathway [1] have been found in different types of cancer, with the highest frequency (more than 50 %) in melanoma and metastatic melanoma [2]. *BRAF* V600 is the most commonly mutated codon, whereby *BRAF* V600E (c.1799T>A) and *BRAF* V600K (c.1798_1799GT>AA)

mutations account for more than 70 and 16 % of the reported mutations, respectively [3].

The FDA-approved drug Vemurafenib is used to treat metastatic melanoma patients bearing an activating *BRAF* V600E mutation, induces tumor regression, and improves overall survival [4] and has also shown to be effective for *BRAF* V600K melanoma patients [5]. The companion FDA-approved cobas® 4800 *BRAF* V600 Mutation Test (Roche Molecular Systems Inc.) allows the detection of the *BRAF* V600E mutation in formalin-fixed paraffin-embedded (FFPE) samples with a limit of detection of ~5 % mutant alleles [6]. It has also shown some ability to detect other V600 mutations, but with a higher detection limit (V600D 10 %, V600K 35 %, and V600E2 65 %) [6]. The low sensitivity of this assay may be problematic in the case of heterogeneous samples with a high contamination of nontumoral DNA or comprising a population of minority clones carrying the mutation [7].

Several other widely used technologies used for *BRAF* V600 mutation detection do also lack sensitivity, while others are more sensitive but do not allow the identification of the mutation [6, 8]. Recently, a wild-type blocking (WTB) PCR assay allowing highly sensitive detection of *BRAF* V600E mutations in FFPE colorectal cancer specimens has been developed with a limit of detection of 0.01 % of mutant alleles [9]. Although the analysis of mutations in circulating DNA is a promising and widely investigated biomarker in different types of cancers including melanoma [10, 11], few methods have been developed for the detection of *BRAF* V600 mutations in cell-free DNA.

Enhanced improved and complete enrichment co-amplification at lower denaturation temperature-polymerase chain reaction (E-*ice*-COLD-PCR) is a novel assay format that allows the highly sensitive mutation detection and identification on fresh frozen and FFPE samples in a single PCR followed by genotyping experiments, within only 3 h [12]. It enables a strong enrichment of the mutation during the PCR where mutant and WT alleles undergo exponential and linear amplification, respectively, due to the introduction of a locked nucleic acid (LNA)-modified blocker probe complementary to the WT sequence [12]. This rapid, easy-to-handle, and cost-effective method can be applied without prior knowledge of the mutation, combines high analytical sensitivity (down to 0.01 %) with the reliable identification of the mutation by (pyro)sequencing, and is potentially suitable for routine use in the clinics [12]. Here, we present the first E-*ice*-COLD-PCR assay for the detection and identification of mutations in *BRAF* codon 600, which is applicable to fresh frozen, FFPE, and also plasma samples.

Methods

BRAF V600 E-*ice*-COLD-PCR assay

Primer and blocker probe design

Primers were purchased from Biotez (Berlin, Germany) and the blocker probe from TibMolBiol (Berlin, Germany). Beacon Designer 8 (Premier Biosoft, Palo Alto, CA, USA) was used to design PCR primers (*BRAF*_121_F: CCTTTACTTACTACACCTCAGATA and *BRAF*_121_R: Biotin-GACAACTGTTCAAACTGATGGGA) which amplify a 121-bp PCR product, while the pyrosequencing primer (*BRAF*_Gen_F: GGTGATTTTGGTCTAGCTAC) was designed with the SNP Primer design software (Qiagen, Courtaboeuf, France). Optimal annealing temperature of primers was determined by a gradient PCR in a Mastercycler Pro S (Eppendorf, Le Pecq, France) and analyzed on a 2 % agarose gel. The 64-base antisense blocker (*BRAF*_64_AS_LNA ATGGGACCCACTCCATCGAGATTT+C+A+CTGTAGCTAGACCAAAATCACCTATTTTTACTGTGAGG-Phosphate) was designed to overlap 6 bases (underlined in the primer and blocker sequences) with the reverse primer (*BRAF*_121_R) and include a triplet LNA bases (marked with a +) on *BRAF* codon 600. The optimal critical temperature of the probe (T_c) for E-*ice*-COLD-PCR was determined as previously described [12].

E-ice-COLD-PCR

E-*ice*-COLD-PCR was performed on a LightCycler 480 thermocycler (Roche Applied Science, Penzberg, Germany). Genomic DNA of 25 pg to 25 ng was used as input in a 25-μL PCR mix including 1× of HotStar Taq DNA polymerase Buffer; 1.6 mM of additional $MgCl_2$; 200 μM of dNTPs; 200 nM of each primer; 2 μM of SYTO9, 20, 30, 50, 70, or 100 nM of the blocker probe (*BRAF*_64_AS_LNA); and 2 U of HotStar Taq DNA polymerase (Qiagen, Courtaboeuf, France). An initial denaturation step was performed for 10 min at 95 °C, followed by 6 cycles of standard PCR (30 s of denaturation at 95 °C, 20 s of annealing at 62 °C, and 10 s of elongation at 72 °C), and 49 cycles of E-*ice*-COLD-PCR (20 s of denaturation at 95 °C; 30 s of blocker annealing at 70 °C and 20 s at 76 °C (T_c); 20 s of primer annealing at 62 °C; and 10 s of elongation at 72 °C) to enrich the mutations. The final step was a melting curve (five acquisitions per degree) from 65 to 95 °C. Instead of a conventional melting curve analysis, a high-resolution melting (20 acquisitions per degree from 65 to 95 °C) could be performed to detect the presence of mutations prior to their identification by sequencing experiments.

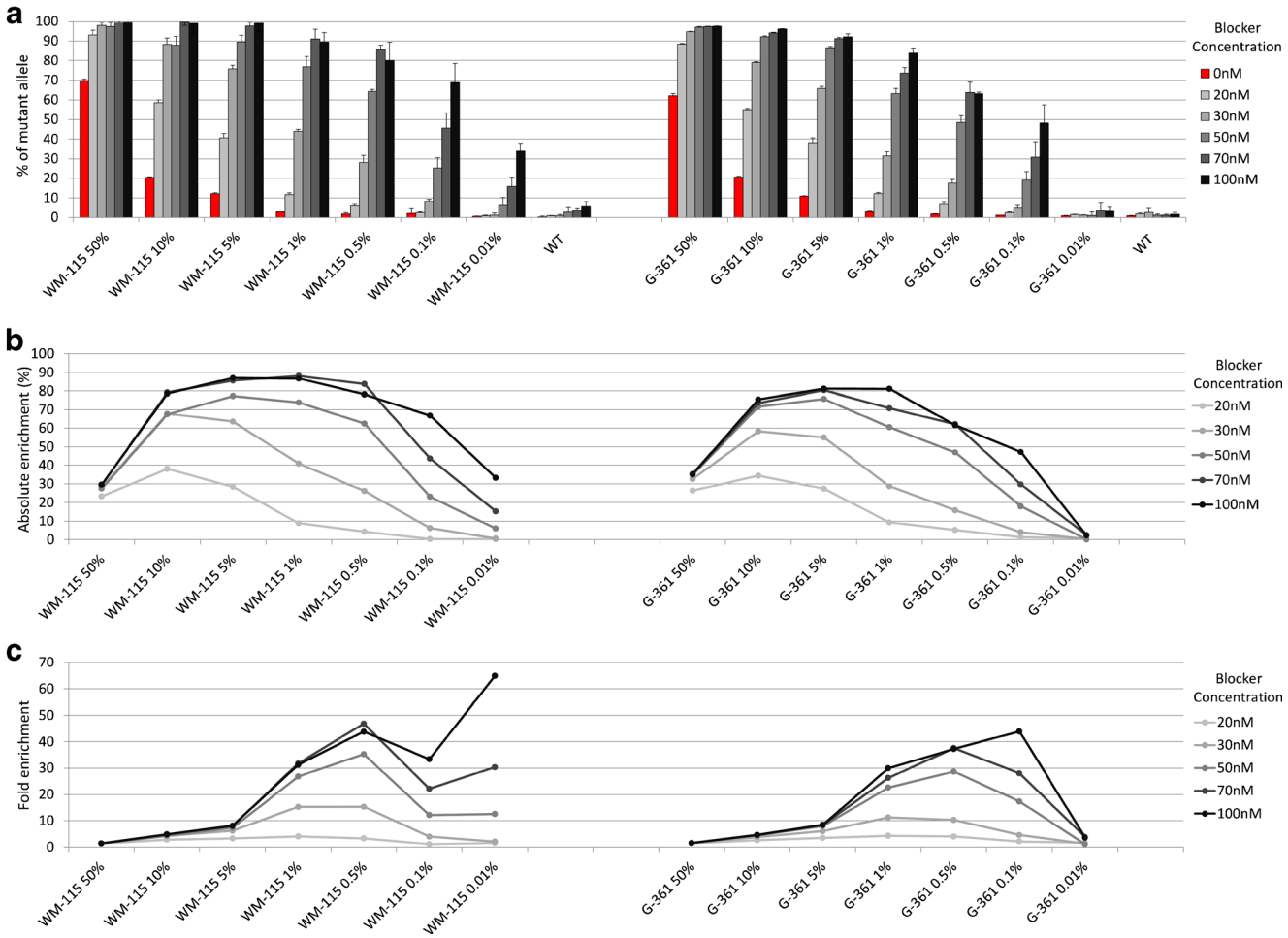

Fig. 1 Quantification of the enrichment of *BRAF* mutations by E-*ice*-COLD-PCR compared to standard PCR using different concentrations of the blocker probe. **a** Quantification of the mutant allele by pyrosequencing after standard PCR (*red*) or E-*ice*-COLD-PCR using different blocker concentrations (*gray scale*). **b** Quantification of the mutation enrichment (in %) after E-*ice*-COLD-PCR compared to a standard PCR calculated by subtracting the mutation percentage obtained after standard PCR from the value of the E-*ice*-COLD-PCR **c** Calculation of the fold enrichment of the mutant allele after E-*ice*-COLD-PCR, i.e., the ratio between the mutation percentage obtained by E-*ice*-COLD-PCR and the value obtained after standard PCR. Numbers after each cell line indicate the percentage of the mutant allele prior to enrichment

The description of the clinical samples as well as additional methods can be found in the online supplementary material (ESM1).

Results and discussion

The development of the assay was performed as previously described, but using a different real-time thermocycler platform [12]. We moved the assay to the LightCycler 480 (Roche Applied Science) for simplicity of the sample preparation and experimental setup compared to a real-time pulsed air thermocycler [12, 13] and its 96-well PCR plate format, making it fully compatible with the downstream pyrosequencing process. On this thermocycler, the critical temperature (T_c) can only be adjusted in increments of 1 °C, but as previously shown, E-*ice*-COLD-PCR, in contrast to other COLD and *ice*-COLD-PCR assays, does not require a very precise T_c [12]. We used pyrosequencing as the sequencing readout is rapid, simple to set up, and allows accurate quantification. For the development of the assay, two cancer cell lines harboring *BRAF* c.1799T>A (V600E, G-361) and c.1799_1800TG>AT (V600D, WM-115) heterozygous mutations were identified (ESM1 Fig. S1). DNA was used in different quantities (25 pg to 25 ng) and different mutation fractions ranging from 50 to 0.01 % in quadruplicate experiments.

A Microsoft Visual Basic Application, available in the electronic supplementary material (ESM1 Fig. S3 and ESM2), based on the analysis of the raw peak intensities of the pyrograms was developed enabling automated and unambiguous identification and quantification of the six most frequent *BRAF* CDS mutations (V600E, V600K, V600R, V600E2, V600D, and K601E) accounting for 95 % of all *BRAF* CDS mutations (COSMIC database; ESM1 Fig. S2). Samples presenting a mutated allele with an allelic ratio of

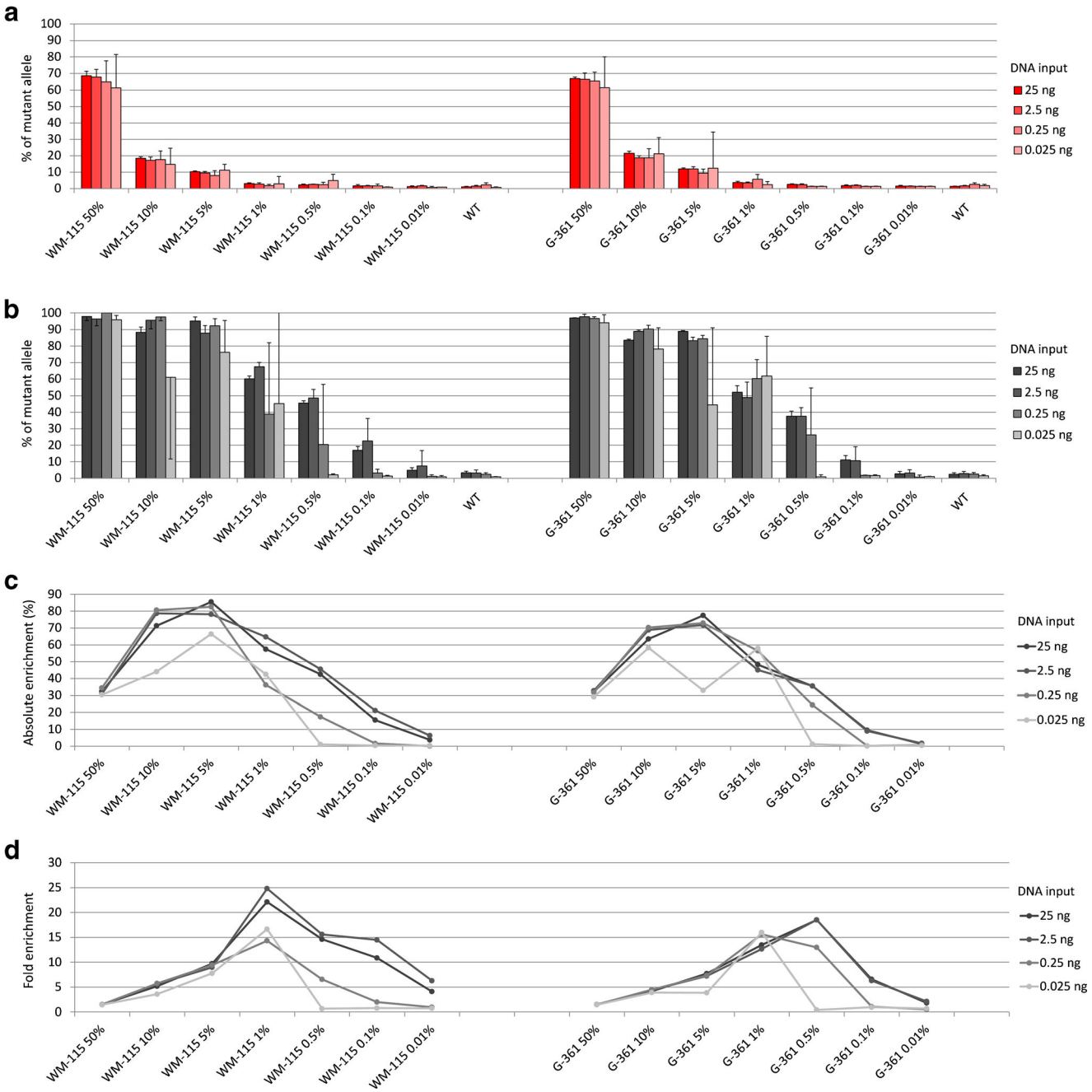

Fig. 2 Quantification of *BRAF* mutation enrichment by E-*ice*-COLD-PCR compared to standard PCR using different low amounts of DNA input to mimic mutation analysis in plasma. **a** Quantification of the mutant allele by pyrosequencing after standard PCR using different amounts of DNA input. **b** Quantification of the mutant allele by pyrosequencing after E-*ice*-COLD-PCR using 40 nM of blocker probes and different amounts of DNA input. **c** Quantification of the mutation enrichment (in %) after E-*ice*-COLD-PCR compared to the value of a standard PCR calculated by subtracting the mutation percentage obtained after standard PCR from the value of the E-*ice*-COLD-PCR. **d** Calculation of the fold enrichment of the mutant allele after E-*ice*-COLD-PCR, i.e., the ratio between the mutation percentage obtained by E-*ice*-COLD-PCR and the value obtained after standard PCR. Numbers after each cell line indicate the percentage of mutant allele prior to enrichment

more than 10 % after enrichment can be reliably considered as mutated according to the quantitative resolution of the pyrosequencer.

When E-*ice*-COLD-PCR was performed using 25 ng of gDNA as the starting amount of template with different concentrations of the LNA blocker probe (20 to 100 nM), a positive dose-effect inhibition of the WT allele was observed resulting in an increased proportion of the mutant allele (Fig. 1a). WT samples could display some background signal after E-*ice*-COLD-PCR depending on the starting amount of blocker probe, but this did not exceed 6 % (100 nM blocker, Fig. 1a). The analytical sensitivity could be increased to 0.1 %

Table 1 *BRAF* mutation detection and identification from fresh frozen (FF), FFPE, and plasma samples of melanomas patients. Sanger sequencing and endpoint genotyping were performed on FF and FFPE samples only. Pyrosequencing after standard PCR and E-*ice*-COLD-PCR were performed on all sample types

Type of sample	Sample	Sanger sequencing	Endpoint genotyping	Standard PCR				E-*ice*-COLD-PCR			
				c.1799T>A	c.1801A>G	Double mutation	Mutation identification	c.1799T>A	c.1801A>G	Double mutation	Mutation identification
FF	1	**V600E**	**V600E**	**45.70**	0.00	0.55	**V600E**	**78.76**	0.00	2.13	**V600E**
FF	2	WT	WT	1.50	0.00	0.86	WT	3.59	0.00	3.93	WT
FF	3	WT	WT	2.40	0.00	0.94	WT	**40.11**	0.00	3.59	**V600E**
FF	4	WT	WT	5.10	0.00	0.95	WT	4.26	0.00	5.16	WT
FF	5	WT	WT	1.26	0.00	3.67	WT	1.57	0.00	3.73	WT
FF	6	**V600E**	**V600E**	**63.15**	0.00	0.46	**V600E**	**95.77**	2.20	1.41	**V600E**
FF	7	**V600E**	**V600E**	**12.41**	0.00	1.10	**V600E**	**79.53**	0.48	2.75	**V600E**
FF	8	**V600E**	**V600E**	**18.10**	0.00	0.62	**V600E**	**85.66**	2.23	1.38	**V600E**
FF	9	**V600E**	**V600E**	**28.40**	0.00	0.88	**V600E**	**95.10**	0.96	1.85	**V600E**
FF	10	**V600E**	**V600E**	**60.25**	0.00	0.89	**V600E**	**95.59**	1.67	0.96	**V600E**
FF	11	**V600E**	**V600E**	**48.90**	0.00	0.69	**V600E**	**93.74**	0.67	1.23	**V600E**
FF	12	**V600E**	**V600E**	**52.24**	0.00	0.77	**V600E**	**95.52**	0.15	1.22	**V600E**
FF	13	**V600E**	**V600E**	**56.68**	0.00	0.63	**V600E**	**97.12**	0.00	1.44	**V600E**
FF	14	**V600E**	**V600E**	**58.21**	0.00	4.34	**V600E**	**94.69**	2.02	1.06	**V600E**
FF	15	**V600E**	**V600E**	**53.26**	0.00	3.52	**V600E**	**94.83**	5.74	1.19	**V600E**
FF	16	**V600E**	**V600E**	**62.98**	0.00	0.63	**V600E**	**79.53**	1.69	0.51	**V600E**
FF	17	**V600E**	**V600E**	**63.64**	0.00	0.51	**V600E**	**80.37**	0.00	0.38	**V600E**
FF	18	**V600E**	**V600E**	**48.16**	0.00	0.60	**V600E**	**69.98**	0.00	1.29	**V600E**
FFPE	19	**V600E**	**V600E**	**20.55**	0.17	1.52	**V600E**	**56.16**	0.00	4.92	**V600E**
FFPE	20	**V600E**	**V600E**	**27.71**	0.00	0.47	**V600E**	**62.19**	0.00	2.89	**V600E**
FFPE	21	**V600D**	WT	Dble mut	Dble mut	**14.12**	**V600D**	Dble mut	Dble mut	**71.06**	**V600D**
FFPE	22	**V600E**	**V600E**	**55.61**	0.00	0.90	**V600E**	**83.45**	0.00	0.81	**V600E**
FFPE	23	**V600E**	**V600E**	**60.07**	0.00	0.86	**V600E**	**84.63**	1.15	1.13	**V600E**
FFPE	24	**V600K**	WT	Dble mut	Dble mut	**56.88**	**V600K**	Dble mut	Dble mut	**86.49**	**V600K**
FFPE	25	**V600E**	**V600E**	**54.80**	0.00	0.39	**V600E**	**75.35**	0.00	3.20	**V600E**
FFPE	26	**V600E**	**V600E**	**48.40**	0.00	1.85	**V600E**	**74.49**	0.00	2.38	**V600E**
FFPE	27	WT	WT	3.62	0.00	1.05	WT	**44.43**	0.00	0.07	**V600E**
FFPE	28	WT	WT	4.36	0.00	0.26	WT	**72.51**	0.00	0.34	**V600E**
FFPE	29	WT	WT	3.85	0.00	1.61	WT	Dble mut	Dble mut	**78.54**	**V600K**
FFPE	30	WT	WT	2.33	0.00	0.61	WT	1.42	0.00	4.55	WT
FFPE	31	WT	WT	1.84	0.00	0.22	WT	3.64	3.15	6.02	WT
FFPE	32	WT	WT	3.29	0.00	1.13	WT	7.21	0.00	7.42	WT
FFPE	33	WT	WT	5.67	0.00	0.50	WT	**53.07**	0.00	5.03	**V600E**
FFPE	34	WT	WT	2.19	0.00	1.83	WT	Dble mut	Dble mut	**53.51**	**V600D**
FFPE	35	WT	WT	6.41	0.00	2.91	WT	**60.12**	0.00	2.06	**V600E**
Plasma	A	–	–	Dble mut	Dble mut	**31.61**	**V600R**	Dble mut	Dble mut	**98.11**	**V600R**[a]
Plasma	B	–	–	3.12	0.00	1.02	WT	0.00	0.00	0.96	WT
Plasma	C	–	–	2.32	0.00	1.22	WT	4.55	0.00	2.36	WT
Plasma	D	–	–	2.93	0.00	0.74	WT	2.46	5.45	0.56	WT
Plasma	E	–	–	2.73	0.00	0.92	WT	**55.47**	0.00	0.51	**V600E**[a]
Plasma	F	–	–	1.98	0.12	0.05	WT	1.17	0.00	2.53	WT
Plasma	G	–	–	1.59	0.67	0.40	WT	1.32	0.00	3.26	WT
Plasma	H	–	–	1.91	0.00	0.79	WT	**14.30**	0.00	4.44	**V600E**[a]
Plasma	I	–	–	1.26	0.00	1.89	WT	1.34	0.00	5.91	WT
Plasma	J	–	–	1.25	0.00	0.95	WT	1.20	0.00	2.60	WT

Table 1 (continued)

Type of sample	Sample	Sanger sequencing	Endpoint genotyping	Standard PCR				E-*ice*-COLD-PCR			
				c.1799T>A	c.1801A>G	Double mutation	Mutation identification	c.1799T>A	c.1801A>G	Double mutation	Mutation identification
Plasma	K	–	–	2.19	0.77	0.53	WT	1.25	0.00	3.09	WT
Plasma	L	–	–	1.69	0.37	0.67	WT	1.33	0.00	2.82	WT
Plasma	M	–	–	1.78	0.00	1.67	WT	1.29	0.08	2.98	WT
Plasma	N	–	–	1.15	0.00	1.70	WT	1.25	0.00	2.80	WT
Plasma	O	–	–	1.69	0.00	0.32	WT	1.25	2.20	3.02	WT
Plasma	P	–	–	2.80	2.43	0.52	WT	2.11	0.00	2.57	WT
Plasma	Q	–	–	1.81	0.00	0.51	WT	1.62	0.00	3.86	WT
NC	WT	–	–	1.40	0.00	1.28	WT	1.41	0.00	4.81	WT
NC	WT	–	–	1.75	0.00	1.44	WT	1.21	0.00	3.40	WT
NC	WT	–	–	1.56	0.00	0.32	WT	2.28	0.67	2.29	WT

The quantification of each type of *BRAF* V600 mutation (c.1799T>A, c.1801A>G, and of double mutations) is expressed in percentage. Mutations with an allelic ratio of more than 10 % (threshold allowing high confidence calls) are shown in bold

NC negative control (mixed human leukocyte DNA)

[a] Plasma samples presenting a positive *BRAF* V600 mutation after E-*ice*-COLD-PCR were also positive in their corresponding tumor sample

for G-361 using 50 nM of blocker and 0.01 % for WM-115 using 70 nM of blocker (Fig. 1a). The highest absolute mutation enrichment (80–90 %) was achieved for both cell lines on the 1 % mutation fraction with 100 nM of blocker (Fig. 1b), whereas the highest fold enrichment (44 for G-361 and 65 for WM-115) was obtained with 100 nM of blocker at the dilution corresponding to the detection limit of each cell line (Fig. 1c). The sensitivity of the assay can be increased to 0.01 % of mutation in a wild-type background which renders our technique as one of the most sensitive assays for *BRAF* V600 mutation detection equaling the sensitivity of the very recently reported WTB-PCR [9]. However, this WTB-PCR blocks completely the amplification of the WT allele thereby prohibiting sequence validation and consumes far more costly LNA blocker compared to E-*ice*-COLD-PCR [9]. Compared to *BRAF* V600 COLD-PCR assays [14, 15], our *BRAF* V600 E-*ice*-COLD-PCR assay presents a lower limit of detection (0.01 % against 3.2 % for *full*-COLD-PCR) and is less sensitive to temperature variation for the critical temperature allowing the use of a 96-well thermocycler. In contrast, E-*ice*-COLD-PCR is associated with a higher cost due to the use of long and chemically modified oligonucleotides and requires a more thorough optimization to determine the right combination of critical temperature and blocker concentration.

To extend the applicability of our assay to circulating DNA isolated from plasma samples, E-*ice*-COLD-PCR was evaluated on decreasing amounts of starting DNA ranging from 25 pg to 25 ng using a fixed amount of blocker probe (40 nM), which was chosen based on the results of the blocker dose effect (Fig. 1). This concentration should yield the required sensitivity (ESM1 Table S1) while not blocking the amplification of the WT allele completely to yield sufficient PCR products for sequencing experiments. After standard PCR, the theoretical mutation ratios were obtained, and this is independent of the dilution and comparable for each mutation fraction tested. However, the standard deviation increased with the dilution of the DNA input and the mutation fraction, reflecting the limiting dilution effect due to a Poisson distribution (Fig. 2a). For E-*ice*-COLD-PCR, an equally efficient enrichment of the mutation was achieved for high mutation fractions (50–10 %) with the different DNA inputs (Fig. 2b). The quantification and its reproducibility displayed increasing variation (shown by increased standard deviations) reflecting also limiting dilution effects with decreasing starting amount of DNA and mutation fraction (Fig. 2b). The analytical sensitivity seemed to decline with the DNA dilution as no mutation enrichment was detected at 0.5, 0.1, and 0.01 % mutation for 25 pg, 250 pg, 2.5 ng, and 25 ng of DNA input, respectively (Fig. 2c, d). However, for low mutation fractions, the probability of the presence of mutated alleles in low DNA input samples must be taken into account, and the absence of enrichment was probably due to the absence of mutated molecules in the analyzed samples (ESM1 Table S1). To confirm this hypothesis, replicate experiments of standard and E-*ice*-COLD-PCR were performed on 25-pg DNA with 5 % mutated alleles. These experiments showed similar enrichment efficiencies compared to the experiments performed on 25 ng of DNA, indicating that E-*ice*-COLD-PCR efficiency is maintained across the DNA dilutions (ESM1 Fig. S4). To achieve the best results in terms of sensitivity and yield of PCR product, we recommend the use of different ranges of blocker probes according to the type of samples, which

present different molecular characteristics (quality and quantity), based on the results obtained using different concentrations of blocker (Fig. 1) or different amounts of DNA inputs (Fig. 2). Thus, for the devised *BRAF* assay, the optimal concentration of the blocker should range between 50 and 100 nM for fresh frozen samples for which a large amount of high-quality DNA is available, 30–50 nM for FFPE where the quality of the DNA is less due to partial degradation, and 20–30 nM for plasma samples available in small quantities not requiring the highest sensitivity. For samples, for which the amount of DNA is not limited, the starting amount of DNA for E-*ice*-COLD-PCR could be increased to above 25 ng as this might allow the use of higher blocker probe concentration to maintain or increase the limit of detection of the technique.

In order to evaluate our assay on different types of samples, standard and E-*ice*-COLD-PCR experiments were performed in duplicate on fresh frozen tumor (n=18), FFPE tumor (n=17), and plasma (n=17) samples from melanoma patients followed by pyrosequencing and compared to Sanger sequencing and endpoint genotyping experiments, with the latter method relying on the same technology as the FDA-recommended diagnostic "cobas® 4800 *BRAF* V600 Mutation Test." After standard PCR, 11 fresh frozen samples, 2 FFPE samples, and 1 plasma sample presented a clear *BRAF* V600 mutation (12–97 %), while all other samples presented a mutation profile comparable to WT samples (Table 1). After E-*ice*-COLD PCR, 12 fresh frozen samples, 8 FFPE, and 3 plasma samples showed *BRAF* V600 mutations (14–97 %) after enrichment (Table 1), identifying 9 additionally mutated samples, 7 of which were also not detected by Sanger sequencing or by endpoint genotyping. E-*ice*-COLD-PCR proved here for the first time to be applicable to clinical plasma samples where it can enrich and detect *BRAF* mutations yielding a sensitivity comparable to allele-specific PCR methods which require separate assays for the different possible mutations [11, 16, 17]. E-*ice*-COLD-PCR is therefore the first sensitive method for *BRAF* V600 mutation detection and identification in a single PCR reaction requiring no prior knowledge on the mutation present in the sample and applicable to circulating DNA from plasma.

Conclusion

In summary, we present an easy-to-implement, highly sensitive method for the detection of the various mutations in *BRAF* codon 600, which can be applied to different sample types and might assist in treatment decision and monitoring, especially using noninvasively obtained sample specimens.

Acknowledgments The authors would like to thank Aurélie Sadoux (AP-HP) and Marie-Pierre Podgorniak (AP-HP) for technical assistance, Leigh Pascoe (CEPH) for his help in statistics, and Steven McGinn (CNG) for the critical reading of the manuscript.

Funding The work in the presented manuscript was funded through the institutional budget of the CEA and the CEPH.

Conflict of interest The authors declare that they have no competing interests.

References

1. Fecher LA, Amaravadi RK, Flaherty KT (2008) The MAPK pathway in melanoma. Curr Opin Oncol 20(2):183–189. doi:10.1097/CCO.0b013e3282f5271c
2. Davies H, Bignell GR, Cox C, Stephens P, Edkins S, Clegg S, Teague J, Woffendin H, Garnett MJ, Bottomley W, Davis N, Dicks E, Ewing R, Floyd Y, Gray K, Hall S, Hawes R, Hughes J, Kosmidou V, Menzies A, Mould C, Parker A, Stevens C, Watt S, Hooper S, Wilson R, Jayatilake H, Gusterson BA, Cooper C, Shipley J, Hargrave D, Pritchard-Jones K, Maitland N, Chenevix-Trench G, Riggins GJ, Bigner DD, Palmieri G, Cossu A, Flanagan A, Nicholson A, Ho JW, Leung SY, Yuen ST, Weber BL, Seigler HF, Darrow TL, Paterson H, Marais R, Marshall CJ, Wooster R, Stratton MR, Futreal PA (2002) Mutations of the BRAF gene in human cancer. Nature 417(6892):949–954. doi:10.1038/nature00766
3. Long GV, Menzies AM, Nagrial AM, Haydu LE, Hamilton AL, Mann GJ, Hughes TM, Thompson JF, Scolyer RA, Kefford RF (2011) Prognostic and clinicopathologic associations of oncogenic BRAF in metastatic melanoma. J Clin Oncol 29(10):1239–1246. doi:10.1200/JCO.2010.32.4327
4. Chapman PB, Hauschild A, Robert C, Haanen JB, Ascierto P, Larkin J, Dummer R, Garbe C, Testori A, Maio M, Hogg D, Lorigan P, Lebbe C, Jouary T, Schadendorf D, Ribas A, O'Day SJ, Sosman JA, Kirkwood JM, Eggermont AM, Dreno B, Nolop K, Li J, Nelson B, Hou J, Lee RJ, Flaherty KT, McArthur GA (2011) Improved survival with vemurafenib in melanoma with BRAF V600E mutation. N Engl J Med 364(26):2507–2516. doi:10.1056/NEJMoa1103782
5. Forschner A, Niessner H, Bauer J, Bender B, Garbe C, Meier F (2013) Successful treatment with vemurafenib in BRAF V600K-positive cerebral melanoma metastasis. JAMA Dermatol 149(5):642–644. doi:10.1001/jamadermatol.2013.372
6. Halait H, Demartin K, Shah S, Soviero S, Langland R, Cheng S, Hillman G, Wu L, Lawrence HJ (2012) Analytical performance of a real-time PCR-based assay for V600 mutations in the BRAF gene, used as the companion diagnostic test for the novel BRAF inhibitor vemurafenib in metastatic melanoma. Diagn Mol Pathol 21(1):1–8. doi:10.1097/PDM.0b013e31823b216f
7. Kristensen T, Clemmensen O, Hoejberg L (2013) Low incidence of minor BRAF V600 mutation-positive subclones in primary and metastatic melanoma determined by sensitive and quantitative real-time PCR. J Mol Diagn 15(3):355–361. doi:10.1016/j.jmoldx.2012.12.003
8. Lade-Keller J, Romer KM, Guldberg P, Riber-Hansen R, Hansen LL, Steiniche T, Hager H, Kristensen LS (2013) Evaluation of BRAF mutation testing methodologies in formalin-fixed, paraffin-embedded cutaneous melanomas. J Mol Diagn 15(1):70–80. doi:10.1016/j.jmoldx.2012.08.003
9. Chen D, Huang JF, Xia H, Duan GJ, Chuai ZR, Yang Z, Fu WL, Huang Q (2014) High-sensitivity PCR method for detecting BRAF V600Emutations in metastatic colorectal cancer using LNA/DNA chimeras to block wild-type alleles. Anal Bioanal Chem 406(9–10):2477–2487. doi:10.1007/s00216-014-7618-x

10. Salvianti F, Pinzani P, Verderio P, Ciniselli CM, Massi D, De Giorgi V, Grazzini M, Pazzagli M, Orlando C (2012) Multiparametric analysis of cell-free DNA in melanoma patients. PLoS One 7(11):e49843. doi:10.1371/journal.pone.0049843
11. Board RE, Ellison G, Orr MC, Kemsley KR, McWalter G, Blockley LY, Dearden SP, Morris C, Ranson M, Cantarini MV, Dive C, Hughes A (2009) Detection of BRAF mutations in the tumour and serum of patients enrolled in the AZD6244 (ARRY-142886) advanced melanoma phase II study. Br J Cancer 101(10):1724–1730. doi:10.1038/sj.bjc.6605371
12. How Kit A, Mazaleyrat N, Daunay A, Nielsen HM, Terris B, Tost J (2013) Sensitive detection of KRAS mutations using Enhanced-ice-COLD-PCR mutation enrichment and direct sequence identification. Hum Mutat 34(11):1568–1580. doi:10.1002/humu.22427
13. Milbury CA, Li J, Makrigiorgos GM (2011) Ice-COLD-PCR enables rapid amplification and robust enrichment for low-abundance unknown DNA mutations. Nucleic Acids Res 39(1):e2. doi:10.1093/nar/gkq899
14. Mancini I, Santucci C, Sestini R, Simi L, Pratesi N, Cianchi F, Valanzano R, Pinzani P, Orlando C (2010) The use of COLD-PCR and high-resolution melting analysis improves the limit of detection of KRAS and BRAF mutations in colorectal cancer. J Mol Diagn 12(5):705–711. doi:10.2353/jmoldx.2010.100018
15. Pinzani P, Santucci C, Mancini I, Simi L, Salvianti F, Pratesi N, Massi D, De Giorgi V, Pazzagli M, Orlando C (2011) BRAFV600E detection in melanoma is highly improved by COLD-PCR. Clin Chim Acta 412(11–12):901–905. doi:10.1016/j.cca.2011.01.014
16. Pinzani P, Salvianti F, Cascella R, Massi D, De Giorgi V, Pazzagli M, Orlando C (2010) Allele specific Taqman-based real-time PCR assay to quantify circulating BRAFV600E mutated DNA in plasma of melanoma patients. Clin Chim Acta 411(17–18):1319–1324. doi:10.1016/j.cca.2010.05.024
17. Aung KL, Donald E, Ellison G, Bujac S, Fletcher L, Cantarini M, Brady G, Orr M, Clack G, Ranson M, Dive C, Hughes A (2014) Analytical validation of BRAF mutation testing from circulating free DNA using the amplification refractory mutation testing system. J Mol Diagn 16(3):343–3499. doi:10.1016/j.jmoldx.2013.12.004